Influence of electrode configuration on the heat transfer performance of a LED heat source

CrossMark

Ing Youn Chen [a], Chien-Jen Chen [a], Chi-Chuan Wang [b],*

[a] Department of Mechanical Engineering, National Yunlin University of Science and Technology, Yunlin 640, Taiwan
[b] Department of Mechanical Engineering, National Chiao Tung University, Hsinchu 300, Taiwan

ABSTRACT

In this study, the effects of electrode configuration on the cooling of LED are presented. A total of six needle type electrodes, including sharp, 0.08, 0.12, 0.37, 0.49 R and flat tip, are used to generate ionic wind for cooling of the LED. The effects of electrode configuration, vertical separation height, and tilt angle on the cooling performance of a LED are reported in this study. It is found that the thermal resistance is reduced with the supplied voltage and a maximum 50% reduction is achieved before the spark-over voltage. For the same supplied voltage, the thermal resistance with a larger vertical separation is also higher. However, the operational range is also longer. The effect of tilt angle on the cooling performance of LED depends on the supplied voltage. With a supplied voltage being less than 6.5 kV, it is found that the thermal resistance is increased when the tilt angle is reduced with a tip radius of 0.12 R. However, the trend is reversed when the supplied voltage is higher than 6.5 kV where the thermal resistance of a smaller tilt angle is lower than that of a larger tilt angle. For the same mesh ground, the effect of electrode configurations cast little influence on the final thermal resistance. All the electrodes show an approximately 50% reduction of thermal resistance in association with its original thermal resistance. However, the corresponding threshold voltage and operational voltage differs significantly. The threshold voltage is lowest for the sharp needle and is increased with the rise of tip radius. On the other hand, the corresponding operational range becomes narrower when the tip radius is increased. Yet the spark-over voltage is also insensitive to change of electrode configuration.

© 2014 Elsevier Ltd. All rights reserved.

1. Introduction

The light-emitting diode (LED) is a semiconductor light source that emits light at a specific wavelength. When compared to fluorescent and incandescent lighting, LEDs feature fast response time, simple structure, environmental benign, vivid colors, high energy efficiency, longevity and easier to put into mass production. Hence, LEDs are gradually replacing traditional light sources in every aspect of lighting applications for its versatile benefits. LED light has a high energy efficiency because the energy of electrons is directly converted to light energy at the p–n junction. However, practical LED converts only 15–30% power input into light, leaving 70–85% energy into heat. The heat dissipation inevitably raises the p–n junction temperature, which decreases the allowable current and optical power. In addition, the lifespan of LED lights decreases when they are exposed to high temperatures for a long period of time. Therefore, effective thermal management of the LED lighting is quite essential to avoid failure of the LEDs [1]. This is because that it had been reported that the optical output of the LED is sharply degraded with the increase in junction temperature because the high temperature significantly influences the reliability and durability of the LED [2]. In contrast to other lighting sources; radiation heat transfer barely contributes to heat dissipation for LED due to its relatively low die temperature as relative to an incandescent lamp [3]. Hence thermal management of LEDs depends mainly on both conduction and convection heat transfer. The former, which determines the thermal resistance from LED junction to substrate, plays essential role in spreading heat from a tiny LED die to its packaging substrate, while the latter is mainly responsible for the heat transfer from substrate to ambient [1].

In practice, passive methods incorporating natural convection heat sinks such as plate fin, pin fin and radial fin (e.g., [4–6]) are mostly adopted for heat transfer augmentation for LED cooling. Yet some active methods such as microjet array cooling, liquid-cooling, thermoelectric cooler, and oscillating heat pipes are also feasible techniques that efficiently dissipate heat out of the high

* Corresponding author. Address: E474, 1001 University Road, Hsinchu 300, Taiwan. Tel.: +886 3 5712121x55105; fax: +886 3 5720634.
E-mail address: ccwang@mail.nctu.edu.tw (C.-C. Wang).

Nomenclature

|			
A	surface area (m^2)	Q_l	heat loss (W)
h	heat transfer coefficient (W m^{-2} K^{-1})	T	temperature difference (K)
k	thermal conductivity (W m^{-1} K^{-1})	R	tip radius (m)
P	LED power input (W)	RH	relative humidity (%)
Q	heat transfer rate (W)	R_{th}	thermal resistance (K W^{-1})
Q_a	actual heat transfer rate (W)		

power LEDs (e.g., [7–10]). Despite the foregoing active methods show effective heat removal in high power LEDs, concerns of noise and vibration resulting from the moving parts of these active methods still prevail. In this regard, rather than using mechanical devices to promote cooling, ionic wind featuring the benefit of forced convection but free of noise concerns is one of the potential candidates [11,12]. This would certainly simplify the design and increase the reliability of the cooling module for LED devices due to the lack of moving parts.

Chen et al. [11] had examined various electrode types, including point, line, and mesh type, on the cooling efficiency of the LED. They showed that the thermal resistance of a LED die can be reduced as much as 50%, yet the point electrode with negative polarity along with the mesh ground electrode gave the best overall cooling performance. In this study, efforts are made further to investigate the configuration of the point electrode on the cooling of LED die. It would be shown later in the investigation that the configuration of the point electrode plays essential role in the operation of cooling of LED.

2. Experimental apparatus and data reduction

The experimental setup consisting of an environmental chamber, a LED die attached on a ceramic substrate, and a power supply
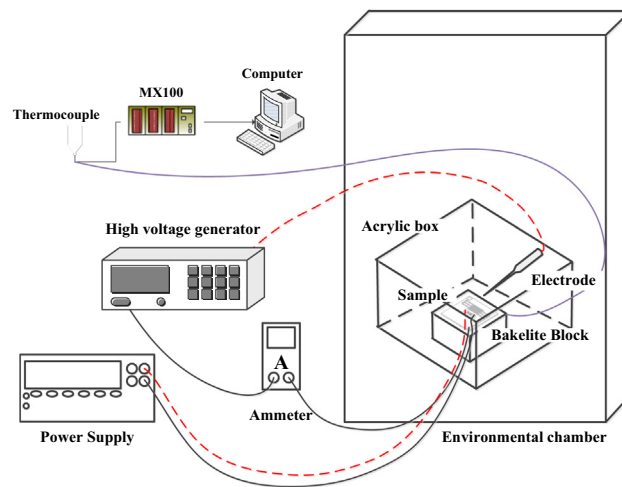
(a) Schematic of the environmental chamber.
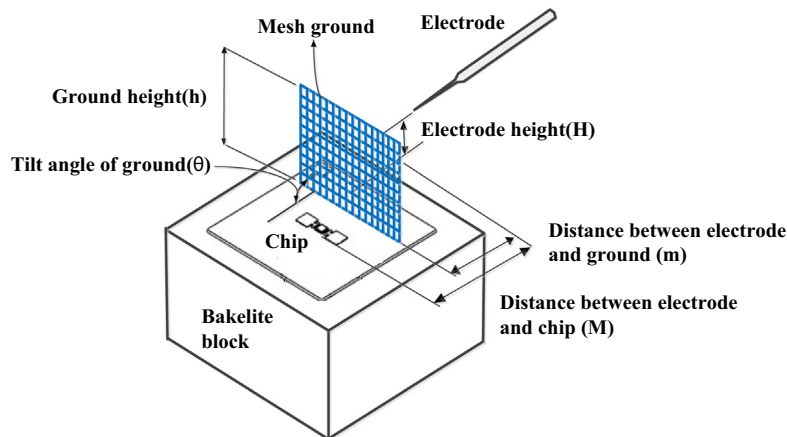
(b) Schematic of test section and the arrangements of electrodes.

Fig. 1. Schematic of the test facility and test section.

system, as well as a data acquisition system, is schematically shown in Fig. 1(a). In order to maintain a constant and uniform ambient temperature throughout the chamber without any fan during the experiment, an environmental chamber having a volume of 0.5 m (L) × 0.5 m (W) × 0.5 m (H) was employed to carry out the experimental tests. The ambient temperature in the chamber was set to be 25 °C and RH = 60% with a controlled resolution of 0.2 °C during the experiment. To minimize the influence airflow within the environmental chamber, an acrylic housing is used to separate the controlled ambient. A power supply (GW Instek GPR-7550D) is used to power the LED and a power meter (Yokogawa WT230) is used to measure the consumed power for those LED. The LED chip size is 0.9 × 0.9 mm having a nominal power consumption of 1 W. Note that the corresponding efficiency of the LED, the ratio of net heat dissipation to total electric power input, is 0.75 according to the luminous efficacy of the present LEDs provided by the manufacturer and the energy balance diagram for high-power white LEDs proposed by Krames et al. [13]. The electrode is placed above the LED as shown in Fig. 1(b). A thermocouple is used to measure the ambient temperature. Besides the ambient temperature measurement, additional five copper–constantan thermocouples (Omega) were used to measure the temperature of the LED chip. Notice that the maximum temperature located at the center is used to calculated the effective thermal resistance of the LED chip. The thermocouples were pre-calibrated from 20 to 80 °C, with a calibrated accuracy of 0.1 °C. All the measured temperatures were recorded by a data acquisition unit (Yokogawa MX100) for further heat transfer analysis. An insulation box made of bakelite with a low thermal conductivity of 0.233 W m^{-1} K^{-1} is placed beneath the heater to reduce the heat loss. In addition, a total of 4 T-type thermocouples are installed inside the bakelite block at two cross positions to calculate the heat loss from the bottom.

The measured average temperature in the bakelite is then used to estimate the heat loss via Fourier's law of conduction. In this study, a point electrode is used for engendering the ionic wind while the mesh ground electrode is used. Notice that the point electrode is made of stainless steel of 1 mm in diameter and capped with various needle tip radius. A total of five needles, including a sharp, a 0.08 R, a 0.12 R, a 0.37 R, a 0.49 R, and a flat needle as shown in Table 1, are used for the measurements. The mesh type electrode is used as the ground. The mesh ground can be set tilt to examine the influence of inclination.

The measured average temperature in the bakelite is then used to estimate the heat loss via Fourier's law of conduction. The heat dissipated of the LED (Q) is estimated as the 75% of the total power input (P) as explained earlier. The actual heat dissipated, Q_a, by convection is thus obtained by subtracting the heat loss (Q_l) from the total dissipated heat:

$$Q_a = Q - Q_l \tag{1}$$

$$Q_l = kA\frac{dT}{dx} \tag{2}$$

where Q_l represent heat loss from the bakelite. The corresponding heat transfer coefficient can be obtained from the Newton's cooling law:

$$h = \frac{Q_a}{A\Delta T} \tag{3}$$

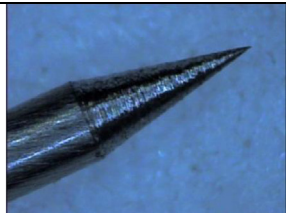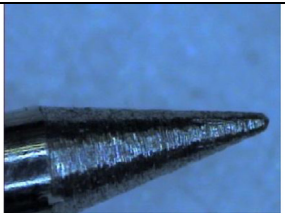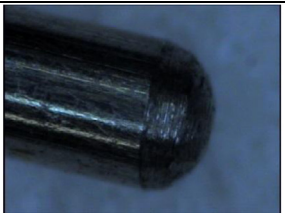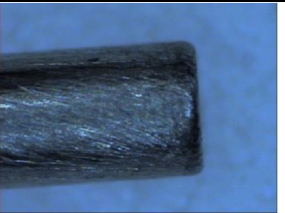Hence, the thermal resistance of the LED subject to EHD is given as:

$$R_{th} = \frac{\Delta T}{Q_a} \tag{4}$$

where ΔT represents the temperature difference between LED and ambient. The uncertainty of the measured thermal resistance was ranged from 3.1% to 6.1%.

3. Results and discussion

Fig. 2(a) shows the effect of aligned ground electrode on the thermal resistance subject to the applied voltage and the corresponding variation of corona current is depicted in Fig. 2(b). The associated tilt angles are 90°, 70°, 45°, and 25° from the horizontal orientation, respectively. Note that the supplied voltage of 0 kV represents the base line reference where only pure natural convection is present. The polarity of the electrode is negative and the tip

Table 1
Photos of the test needle electrodes.

| Sharp need | Needle tip with 0.08 R | Needle tip with 0.12 R |
| Needle tip with 0.37 R | Needle tip with 0.49 R | Flat needle |
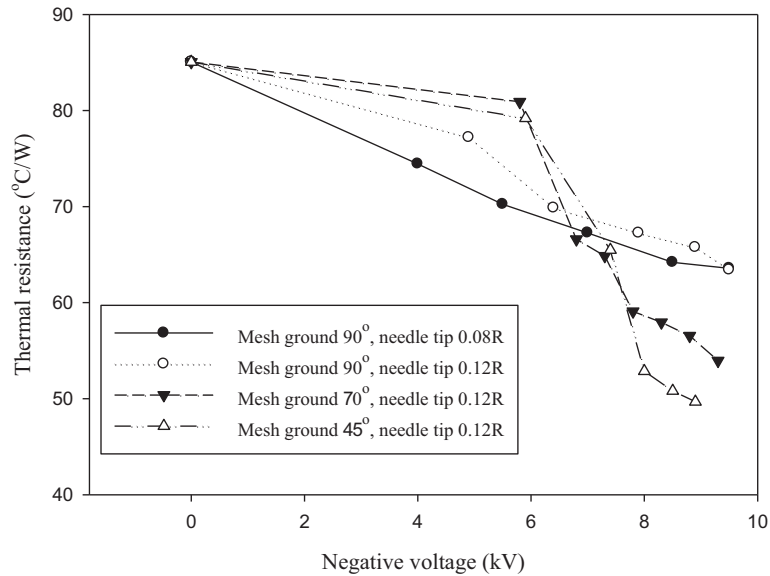
(a) Thermal resistance vs. supplied voltage.
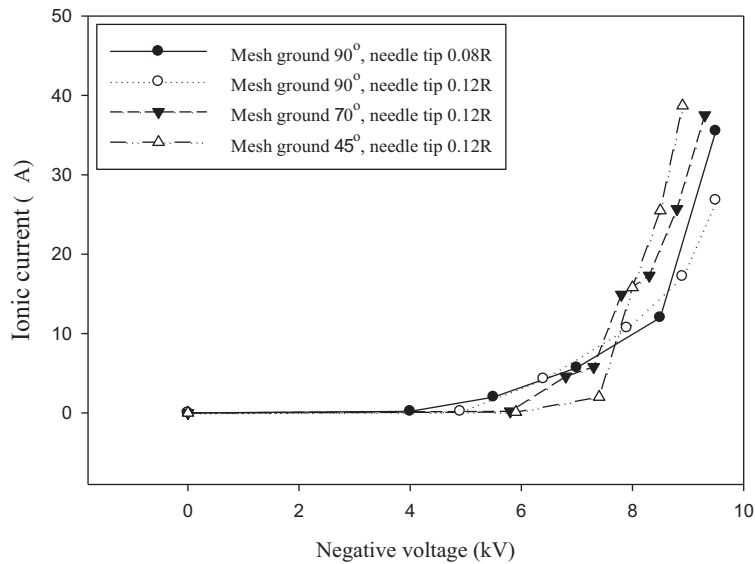
(b) Ionic current vs. supplied voltage.

Fig. 2. Effect of aligned ground electrode on the cooling of LED die with vertical distance 5 mm and horizontal distance 10 mm between the point electrode and mesh ground.

radii are 0.08 and 0.12 R, respectively. The height of the point electrode is 5 mm above the LED substrate whereas the ground electrode is located on the substrate having a mesh configuration as shown in Fig. 1(b). Test results clearly show that the thermal resistance is reduced with the rise of the applied voltage as long as the supplied voltage pass over the threshold voltage, and the maximum reduction in thermal resistance can be as high as 50% before the spark over voltage is reached. The test results are in line with the previous study [11] in which a maximum 50% reduction of the thermal resistance relative to natural convection was also reported. For the same tilt angle of 90°, the thermal resistance for 0.08 R is lower than those of 0.12 R. We will defer the discussion of the configuration of electrode in subsequent discussion. For the electrode with a tip radius of 0.12 R, it appears that the effect of tilt angle is subject to the operational voltage. When the

supplied voltage is lower than 6.5 kV, it is found that the thermal resistance is increased when the tilt angle is reduced. However, the trend is reversed when the supplied voltage is higher than 6.5 kV where the thermal resistance of a smaller tilt angle is lower than that of a larger tilt angle. The results can be made clear from the corresponding ionic current depicted from Fig. 2(b). With a lower tilt angle, the effective distance between the point electrode and the ground mesh is longer, thereby the associated threshold voltage is delayed to approximate 6 kV for a tilt angle of 70° and to about 6.5 kV for a tilt angle of 45°. In this regard, the exerted ionic wind is expected to be smaller than that of a tilt angle of 90°. As a consequence, the thermal resistance for the vertical arrangement is better that those having lower tilt angle. However, once the threshold voltage is initiated for a lower tilt angle, it appears that the corresponding ionic current rises considerably

and eventually shows a similar magnitude as that of the vertical one, implying a similar strength of the engendered ionic wind. However, the tilt arrangement suggests that the induced air flow may flow towards the LED die and give rise to a better heat transfer performance. As a consequence, the trend is reversed when the supplied voltage passes 6.5 kV. The airflow produced by electronic discharge in a pin-plate configuration was numerically illustrated by Zhao and Adamiak [14]. They had conducted a numerical calculation of the airflow engendering from a needle electrode normal to a plate ground. Their calculations clearly show that an apparent axial flow is induced from the electrode toward the plate ground while a radial flow component occurs near the ground plate, and a re-circulation may even exist from this radial component. With the rise of the aligned angle, it is expected that the radial component is also increasing which may contribute to reduce the thermal resistance. But on the other hand, a further rise of aligned angle

also reduce the axial velocity component that acts to increase the thickness of thermal boundary layer and the possible formation of re-circulation of the radial component as shown by Zhao and Adamiak [14].

For a further examination of the influence of the location of electrode above the substrate, experiments with the vertical height distance of 5, 10, 15, 20, and 25 mm above the substrate are conducted for comparison. The corresponding tilt angle of the ground electrode is 70°. Test results in terms of thermal resistance and consumed power is shown in Fig. 3. Basically, a shorter distance between the electrode and substrate leads to an early initiation of the ionic wind and result in a lower thermal resistance. However, the corresponding higher electrical strength also leads to an early spark over voltage, indicating a shorter operational range. Thus, the maximum thermal resistance reduction is about 80% for a height of 5 mm. On the other hand, increasing the height also
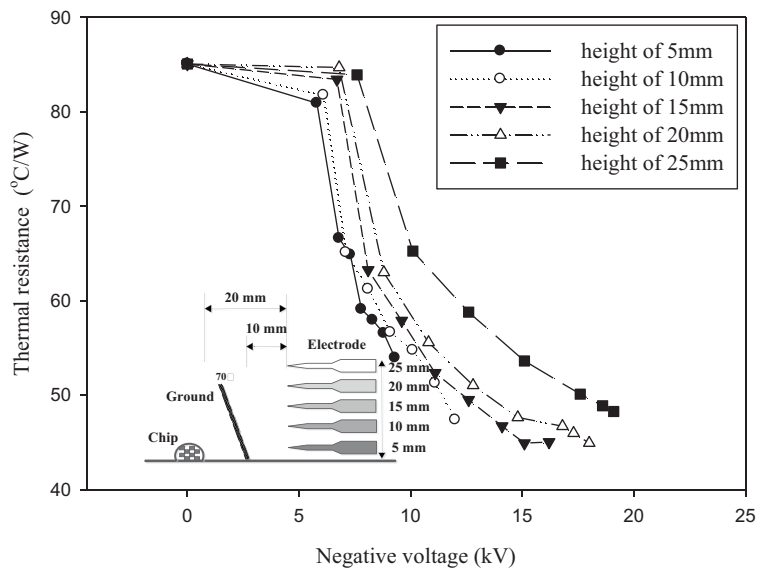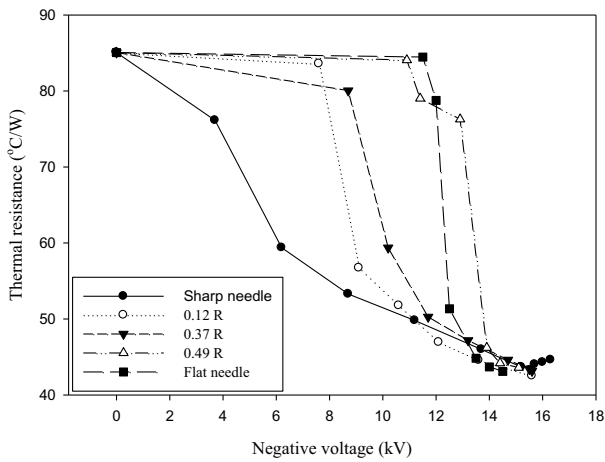

(a) Thermal resistance vs. supplied voltage.
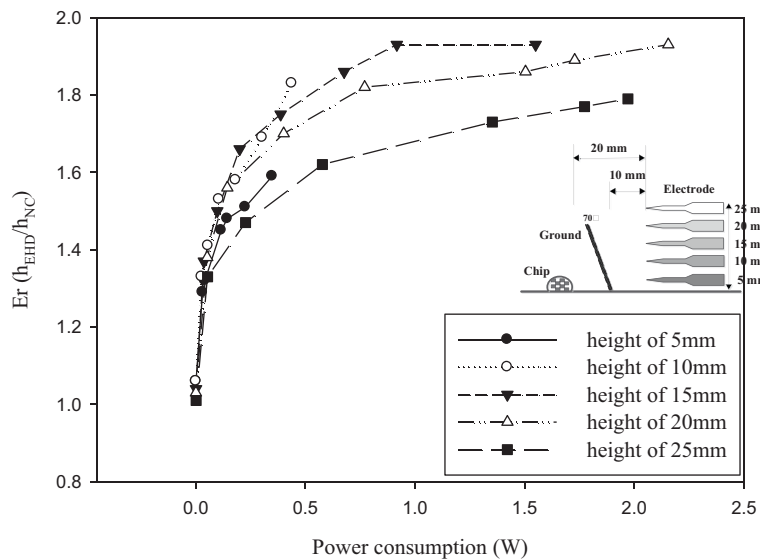


(b) Enhanced ratios vs. consumed power.

Fig. 3. Effect of electrode height on the cooling of LED die; the mesh ground is 70° tilt from the horizontal.

brings about longer operational range but it also accompanies with a much slower reduction in thermal resistance when the supplied voltage is raised. This phenomenon is similar to the aforementioned discussion. The axial velocity flowing along the substrate for a shorter vertical separation distance is apparently higher when compared to those having higher heights. Despite the operational range can be increased when the vertical distance is increased, the related power consumption is also increased considerably due to its much higher operational voltage as shown in Fig. 3(b). From Fig. 3(b), the associated heat transfer augmentation is higher for a shorter vertical separation distance at a given power. In summary of the foregoing discussion, it is suggested a vertical separation distance of 15–20 mm for the placement of the electrode is recommended. This is because it provides a sufficient reduction of thermal resistance (∼90%) and can be operated with an appreciable range.
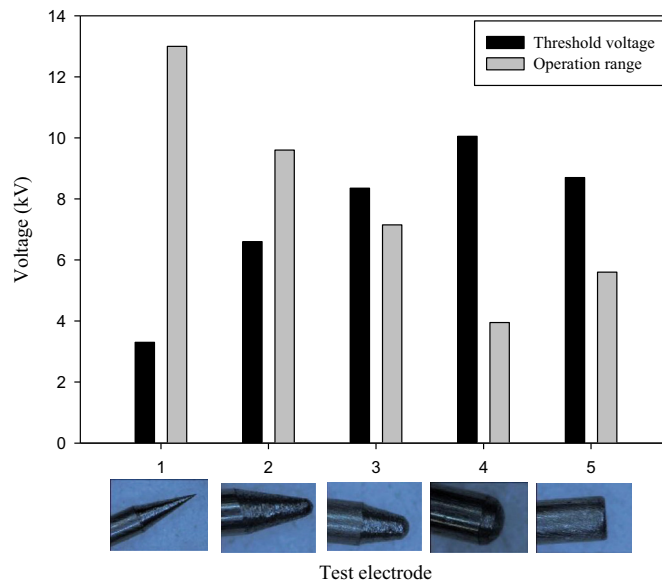
The effect of electrode configuration on the overall performance of the LED cooling is shown in Fig. 4. Again, the corresponding tilt angle is 70° and the height of electrode is 15 mm. From Fig. 4(a), one can see the final reduction of thermal resistance is about 50% regardless the electrode configurations when the supplied voltage is around 14–16 kV. The final spark over voltage is roughly the same for all the five electrode configurations. The results indicate that the break down voltage is almost independent of the configurations of electrode. This is somehow expected for the ground electrode remains the same for all the electrode configurations. Rickard et al. [15] had shown that the break-down voltage is more related to the ground electrode. Despite the final reduction of the thermal resistance is about then same, it appears that the decline trend of the thermal resistance against the supplied voltage is totally different for the five configurations. For the sharp needle, a lower threshold voltage and a steady decrease of the thermal resistance

(a) Thermal resistance vs. supplied voltage.
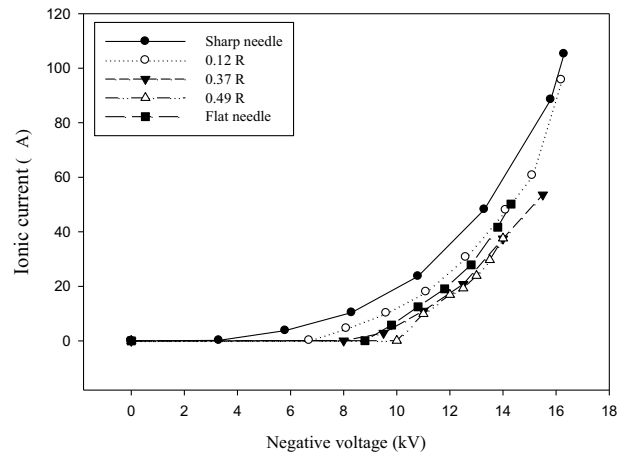
(b) Ionic current vs. supplied voltage.

(c) Threshold voltage/Operational Range for various configurations of electrode.

Fig. 4. Effect of electrode configuration on the performance of LED cooling.

with the supplying voltage is encountered. This is because the electrical potential is more intense and concentrated for a sharp needle configuration, thereby resulting in a comparatively strong ionic wind. With the rise of tip radius of the electrode, the corresponding threshold voltage for effective initiation of the ionic wind is delayed. The strength of ionic wind is resulted from ionization and acceleration. Larger electrical potential caused by sharper configuration at the electrode will give rise to these two consequences. With a sharper needle tip, the electrical field in the vicinity of the electrode is raised considerably that provide a sufficient potential to ionize the particles which then is accelerated towards the ground electrode. Consequently, it results in an early threshold voltage for a sharper configuration. This can be made clear from the measured ionic current shown in Fig. 4(b) which indicates that the sharper configuration provides a larger ionic current. The results agree with the research carried out by Adamiak and Atten [16] who performed numerical simulations of point electrodes having $R = 95$ μm and $R = 35$ μm. Their calculations shows that the onset of ionic wind for $R = 35$ μm is about 20% lower than those of $R = 95$ μm. In the meantime, as shown in the figure, the decline of thermal resistance becomes more pronounced once the initiation starts, indicating a faster rise of ionic current. Moreover, this phenomenon becomes even more pronounced as the radius of the point electrode is increased to 0.49 R whose corresponding threshold voltage is as high as 12 kV. The results suggest that the operational range of the electrode, termed as the difference between the threshold and breakdown voltage, is reduced when the tip radius is increased. For a detailed comparison, the corresponding threshold voltage and operational range for all the configurations is shown in Fig. 4(c). The threshold voltage is defined as the voltage where the thermal resistance is reduced by 5% when compared to the reference state (natural convection only). As shown in the figure, the threshold voltage increases with the tip radius while the operational range decreases with it. One exception is the needle electrode with flat surface which shows a slightly lower threshold voltage and a higher operational range in association with those of 0.49 R. This is due to the edge effect of the flat surface. The related edge provides a similar effect of sharp electrode to a lesser strength.

4. Conclusions

This study examines the enhancement of LED cooling effect via ionic wind subject to various electrode configurations. A total of six needle type electrodes are examined. The shape of the electrode is basically a needle configuration but with different rounding on the tip, including a sharp, a 0.08 R, a 0.12 R, a 0.37 R, a 0.49 R and a flat tip. The needle type electrode having negative polarity is used to generate ionic wind and the operated voltages ranges from 3 to 17 kV. The nominal rated power is of the LED (0.9 × 0.9 mm) is 1 W. The effects of electrode configuration, vertical separation height, and tilt angle on the cooling performance of the LED are reported. Based on the test results, the following conclusions are made:

(1) The thermal resistance is reduced with the rise of supplying voltage, and a maximum 50% reduction is achieved before the spark-over voltage. For the same supplied voltage, the thermal resistance for a larger vertical separation is also higher. However, the operational range is also wider before the spark-over voltage, and it may also accompany with a slightly lower thermal resistance.

(2) The effect of tilt angle on the cooling performance of LED depends on the supplied voltage. When the supplied voltage is less than 6.5 kV for an electrode having a tip radius of 0.12 R, it is found that the thermal resistance is increased when the tilt angle is reduced. However, the trend is reversed when the supplied voltage is higher than 6.5 kV where the thermal resistance of a smaller tilt angle is lower than that of a larger one.

(3) For the same mesh ground, the effect of electrode configurations casts a negligible influence on the final thermal resistance. All electrodes can provide an approximately 50% reduction of the thermal resistance. However, the corresponding threshold voltage and operational voltage varies considerably. The sharp needle gives the lowest threshold voltage and the threshold voltage increases steadily with the tip radius. On the other hand, the corresponding operational range becomes narrower when the tip radius is increased. In addition, the spark-over voltage is also insensitive to change of electrode configuration.

Conflict of interest

None declared.

Acknowledgment

References

[1] A. Christensen, S. Graham, Thermal effects in packaging high power light emitting diode arrays, Appl. Therm. Eng. 29 (2009) 364–371.
[2] N. Narendran, Y. Gu, Life of LED-based white light sources, IEEE/OSA J. Disp. Technol. 1 (1) (2005) 167–170.
[3] J. Petroski, Spacing of high-brightness LEDs on metal substrate PCB's for proper thermal performance, in: Thermomechanical Phenomena in Electronic Systems in proceedings of the Intersociety Conference, 2004.
[4] J.C. Shyu, K.W. Hsu, K.S. Yang, C.C. Wang, Thermal characterization of shrouded plate fin array on an LED backlight panel, Appl. Therm. Eng. 31 (2012) (2012) 2909–2915.
[5] R.T. Huang, W.J. Sheu, C.C. Wang, Effect of orientation on the natural convective performance of square pin fin heat sinks, Int. J. Heat Mass Transfer 51 (2008) 2368–2376.
[6] D. Jang, S.H. Yu, K.S. Lee, Multidisciplinary optimization of a pin–fin radial heat sink for LED lighting applications, Int. J. Heat Mass Transfer 55 (2012) 515–521.
[7] Y. Lai, N. Cordero, F. Barthel, F. Tebbe, J. Kuhn, R. Apfelbeck, D. Wurtenberger, Liquid cooling of bright LEDs for automotive applications, Appl. Therm. Eng. 29 (2009) 1239–1244.
[8] Y. Deng, J. Liu, A liquid metal cooling system for the thermal management of high power LEDs, Int. Commun. Heat Mass Transfer 37 (2010) 788–791.
[9] Z.M. Wan, J. Liu, K.L. Su, X.H. Hu, S.S. M, Flow and heat transfer in porous micro heat sink for thermal management of high power LEDs, Microelectronics 42 (2011) 632–637.
[10] J. Li, B. Ma, R. Wang, L. Han, Study on a cooling system based on thermoelectric cooler for thermal management of high-power LEDs, Microelectron. Reliab. 51 (2011) 2210–2215.
[11] I.Y. Chen, M.Z. Kuo, K.S. Yang, C.C. Wang, Enhanced cooling for LED lighting using ionic wind, Int. J. Heat Mass Transfer 56 (2013) 285–291.
[12] W.J. Sheu, J.J. Hsiao, C.C. Wang, Effect of oscillatory EHD on the heat transfer performance of a flat plate, Int. J. Heat Mass Transfer 61 (2013) 419–424.
[13] M.R. Krames, O.B. Shchekin, R. Muller-Mach, G.O. Muller, L. Zhou, G. Harbers, G. Craford, Status and future of high-power light-emitting diodes for solid-state lighting, J. Disp. Technol. 3 (2007) 160–175.
[14] L. Zhao, K. Adamiak, EHD flow in air produced by electrical corona discharge in pin-plate configuration, J. Electrostat. 63 (2005) 337–350.
[15] M. Rickard, D. Dunn-Rankin, F. Weinberg, F. Carleton, Maximizing ion-driven gas flows, J. Electrostat. 64 (2004) 368–376.
[16] K. Adamiak, P. Atten, Simulation of corona discharge in point-plane configuration, J. Electrostat. 61 (2004) 85–98.